

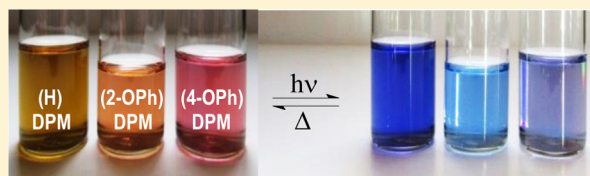
Synthesis and Kinetics of Sterically Altered Photochromic Dithizonatomercury Complexes

Ernestine Alabaraoye, Karel G. von Eschwege,* and Nagarajan Loganathan

Department of Chemistry, University of the Free State, P.O. Box 339, Bloemfontein 9300, South Africa

S Supporting Information

ABSTRACT: Following a previous study where 12 electronically altered dithizones were synthesized, here we report on attempts to synthesize 26 dithizones. The purpose was to explore the boundaries within which dithizones may be synthesized, explore spectral tuning possibilities, and investigate steric effects on the photochromic reaction of its mercury complexes. Contrary to expectation, large substituents like phenoxy groups increased the rate of the photochromic back-reaction. In the series H-, 2-CH₃-, 4-CH₃-, 3,4-(CH₃)₂-, 2-OC₆H₅-, and 4-OC₆H₅-dithizonatophenylmercury(II), the lowest rate of 0.0004 s⁻¹ was measured for the 2-CH₃ complex, while the rate for the 2-OC₆H₅ derivative was 20 times higher. A solvent study revealed a direct relationship between dipole moment and the rate of the back-reaction, while the relationship between temperature and rate is exponential, with $t_{1/2} = 2 \text{ min } 8 \text{ s}$ for the 4-phenoxy complex. The crystal structures of two dithizone precursors, 2-phenoxy- and 4-phenoxy-nitroformazan, are reported.



1. INTRODUCTION

Around 1950, Irving¹ and Webb² independently observed photochromic behavior in the bis-dithizonatomercury(II) complex, Hg(HDz)₂. The reaction entails photoinduced isomerization around the $\text{C}=\text{N}$ bond, switching from the orange resting state to the blue photoinduced new ground state³ (see Figure 2). A photon of blue-green light excites the HOMO electron to the S₁ energy state, which is followed by rotation to the 90° orthogonal geometry energy minimum, where relaxation through the conical intersection is followed by bifurcation—partially back to the orange ground state and partially onward to the blue photoinduced state.⁴ The thermal back-reaction is a radiationless process, the rate of which is determined by the temperature, metal, ligand substituent, medium, and the presence of impurities. The half-life of the blue state may vary from fractions of a second to minutes.

In 1965, Meriwether et al. conducted the first kinetic studies involving this reaction,^{5,6} which were followed up only recently, in 2013.⁷ In the latter study the effects of concentration, solvent, temperature, and electronically altered substituents on the return reaction of photochromic dithizonatophenylmercury(II) (DPM) were kinetically investigated. A complete study of the ultrafast forward reaction involving the same series was subsequently reported in 2014.⁸ Interestingly, from these studies it was found that the 2-CH₃ derivative of DPM has the fastest blue-state population time ($\tau = 1.7 \text{ ps}$), while at the same time its spontaneous back-reaction is the slowest ($t_{1/2} = 58 \text{ min}$). The 4-SCH₃ derivative conversion to its blue form, in turn, was the slowest ($\tau = 3.6 \text{ ps}$), while its back-reaction gave $t_{1/2} = 7 \text{ min}$.

To extend the former kinetic studies, we now report on the following:

- broadened syntheses, mainly to *sterically* alter the ligand, whereby also the aromatic ring system in the ligated complex may be expanded;
- the effects of these changes, as well as concentration, solvent, and temperature, on the kinetics of the photoinduced color-switching back-reaction; and
- accompanying X-ray structural work involving two nitroformazan reaction intermediates.

Data from all these studies build a platform of basic understanding on the present class of photoactive compounds, which have potential applications in new energy conversion technologies. Together with solvatochromism and concentration chromism observed for the dithizone free ligand,⁹ electrochromism^{10,11} and photochromism in its metal complexes provide a mix of interesting properties for ongoing research.

2. EXPERIMENTAL SECTION

2.1. General. Reagents purchased from Sigma-Aldrich and solvents from Merck were used without further purification. The ¹H NMR spectra were recorded on a 300 MHz Bruker DPX 300 NMR spectrometer (298 K). UV–visible spectra of dilute solutions in optical glass cuvettes were recorded on a Shimadzu UV-2550 spectrometer fitted with a Shimadzu CPS temperature controller, while photoexcitation of the photochromic mercury complexes was achieved with a 400 W mercury-halide lamp. A Bruker X8 APEXII 4K Kappa CCD diffractometer was used for single crystal data collections.

2.2. Synthesis. Syntheses of the DPM series employed commercially available substituted (R) anilines as starting

Received: July 29, 2014

Revised: October 22, 2014

Published: October 23, 2014



reagents, proceeding via the nitroformazan intermediates (see Table 1) to the dithizone ligands, and finally complexing with phenylmercury(II) chloride.⁷

Table 1. Yields, Melting Points, and UV–Visible Absorbance Maxima in Acetone of Products Resulting from the Nitroformazan Synthesis Step (R = Substituent, R' = Phenyl Replacements)

R	yield (%)	mp (°C)	λ_{\max} (nm)
H	68	130	445
2-OH	69	210	422
3-OH	52	194	423
4-OH	79	>230	470s
2-SH	62	86	378s
3-SH	70	108	418
4-SH	68	>230	461
2-NO ₂	76	117	360s
3-NO ₂	72	116	487
4-NO ₂	77	126	607
2-CF ₃	67	95	422s
3-CF ₃	64	oil	
2-CH ₃	73	144	457
4-CH ₃	84	150	455
3,4-(CH ₃) ₂	72	162	447
2,4,6-(CH ₃) ₃	72	127	350
2,4,6-(C(CH ₃) ₃) ₃	0		
2,6-(CH ₂ CH ₃) ₂	68	oil	
2-COCH ₃	39	oil	
2-OC ₆ H ₅	81	169	469
4-OC ₆ H ₅	79	137	467
1,2-NHCH ₃	63	154	439
1,4-NHC ₆ H ₅	49	121	456
R' = naphthyl	76	159	508
R' = anthracenyl	51	>230	450
R' = pyrenyl	6	>230	498

Characterization data of dithizones and its mercury complexes which were successfully synthesized and not previously reported⁷ are given below.

2-Phenoxydithizone. Nitroformazan yield: 81%, mp 169–170 °C, λ_{\max} /nm (acetone) 469. Dithizone yield: 98%, mp 173–174 °C, λ_{\max} /nm (acetone) 465 and 637. ¹H NMR (300 MHz, CDCl₃): δ 6.94–8.08 (18 H, m, 2×C₆H₄OC₆H₅), 13.07 (2 H, s, 2×NH).

2-Phenoxydithizonatophenylmercury(II). Yield: 82%, mp 131–132 °C, λ_{\max} /nm (acetone) 482. ¹H NMR (300 MHz, CDCl₃): δ 6.76–7.86 (23 H, m, 2×C₆H₄OC₆H₅ and 1×C₆H₅), 9.60 (1 H, s, 1×NH). Product is photochromic.

4-Phenoxydithizone. Nitroformazan yield: 79%, mp 137–138 °C, λ_{\max} /nm (acetone) 467. Dithizone yield: 60%, mp 114–115 °C, λ_{\max} /nm (acetone) 455 and 634. ¹H NMR (300 MHz, CDCl₃): δ 7.10–7.67 (18 H, m, 2×C₆H₄OC₆H₅), 12.53 (2 H, s, 2×NH).

4-Phenoxydithizonatophenylmercury(II). Yield: 86%, mp 173–174 °C, λ_{\max} /nm (acetone) 486. ¹H NMR (300 MHz, CDCl₃): δ 6.98–7.94 (23 H, m, 2×C₆H₄OC₆H₅ and 1×C₆H₅), 9.20 (1 H, s, 1×NH). Product is photochromic.

Naphthylidithizone. Nitroformazan yield: 76%, mp 158–159 °C, λ_{\max} /nm (acetone) 508. Dithizone yield: 75%, mp 188–189 °C, λ_{\max} /nm (acetone) 492 and 670. ¹H NMR (300 MHz,

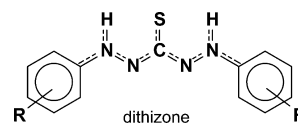
CDCl₃): δ 7.65–8.41 (14 H, C₁₀H₇, 2×C₁₀H₇), 13.60 (2 H, s, 2×NH).

Naphthylidithizonatophenylmercury(II). Yield: 79%, mp 230–231 °C, λ_{\max} /nm (acetone) 489. ¹H NMR (300 MHz, CDCl₃): δ 6.80–8.70 (19 H, m, 2×C₁₀H₇ and 1×C₆H₅), 10.06 (1 H, s, 1×NH). The product is *not* photochromic.

3. RESULTS AND DISCUSSION

3.1. Synthesis. The synthesis of a wide range of chemically altered dithizones was attempted in this study. Although the primary aim was to investigate the effect of steric alterations on the photochromic reaction of its mercury complexes, a secondary aim was to further explore the dithizone synthesis boundaries that may limit future research in this field.

The method that was used brought about symmetrically substituted dithizones, i.e., with substituents similarly placed on both phenyl rings of the ligand. The 26 anilines listed in Table 1 were employed as starting reagents. This series also included naphthyl, anthracenyl, and pyrenyl moieties, which did not serve as substituents but in fact replaced the entire dithizone phenyl groups.

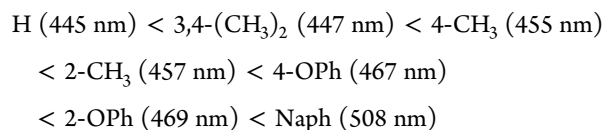


The first step nitroformazan synthesis method proved to be largely successful. Synthesis of the 2,4,6-tri-*tert*-butyl derivative was the only outright failure, which may be ascribed to steric hindrance imposed by the two large *ortho*-placed *tert*-butyl substituents. Yields of all the other products ranged from about 50% to almost 90%, with the 4-methyl derivative giving the highest yield of 88%, and the 4-NH-phenyl derivative yielding 49%. The exception was with the huge pyrenyl compound, where the nitroformazan yield was only 6%.

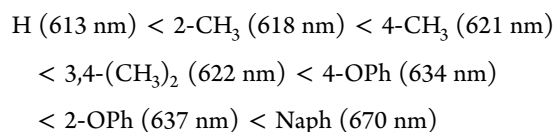
Traditionally, the precipitated orange-red nitroformazans gave absorbance maxima at ca. 445–470 nm, as also seen for the above methyl-substituted derivatives, 4-OH and -SH, 3-NO₂, 2- and 4-OC₆H₅, 1,4-NHC₆H₅, and the anthracenyl compound, i.e., widely indicative of the desired products. A bathochromic shift of about 40 nm is seen for the naphthyl-nitroformazan, to 508 nm. In contrast, a large hypsochromic shift was observed for 2,4,6-trimethylnitroformazan, namely to λ_{\max} = 378 nm. As in the case of 2,6-diethylnitroformazan, a red-brown oil was obtained.

From the list of seven main compounds, i.e., the derivatives that were successfully synthesized right through to its mercury complexes, the following increasing order in wavelengths at maximum absorbances is seen:

Nitroformazans:



Dithizones:



A mostly similar order is observed for both the nitroformazan and dithizone series, with some exception among the few methylated compounds. The naphthyl dithizone again, as for its nitroformazan, shows a large red-shift to 670 nm with respect to the 613 nm of unsubstituted dithizone.

In the second part of the synthesis procedure, addition of ammonium sulfide exchanged the nitro group for sulfur while reducing the compound to the thiocarbazine, H_4Dz . By addition of methanolic potassium hydroxide, H_4Dz was then deprotonated to the orange-red potassium dithizonate salt, K^+HDz^- . The dithizone product, H_2Dz , was finally precipitated by addition of dilute hydrochloric acid.

During the latter steps, the yields of more than half the series dropped, even right down to zero. As for the methylated compounds, dithizone yields decreased from 2-methyl, 4-methyl, and 3,4-dimethyl to the 2,4,6-trimethyl derivative by 74, 30, 13, and 0%, respectively. Both the increasing steric hindrance posed by the increasing number of methyls on both phenyl rings, and the accompanying subtle increase in electron density on the molecular backbone, are proposed to contribute toward the drastic yield decrease that was observed. In contrast, a very high yield of 98% was obtained for the 2-phenoxy dithizone.

Of the extended ring series, syntheses of the naphthyl- and anthracenyl dithizone were successful; however, as yet this may not be said with absolute surety about the latter. Traditionally, all dithizones have been intensely deep green, but the anthracenyl product had an intense deep purple color. During repeated column purifications, similar *different* color lines appeared on the column, indicating an unstable anthracenyl compound that decomposed during chromatography. Also, extensive ongoing efforts to grow crystals suitable for X-ray crystallography have, to date, been unsuccessful.

A number of compounds formed a dark tar/oil, especially in one of the very last two steps (i.e., the base or acid treatment steps), or otherwise simply did not yield a product that had the typical intense color of dithizone. Among these were the 2,4,6- $(CH_3)_3$, 2,6- $(C_2H_5)_2$, and 2- NO_2 compounds, all the OH and SH derivatives, and the 2-COCH $_3$, 2- and 3-CF $_3$ as well as the 2-NHCH $_3$ and 4-NHC $_6H_5$ compounds. After repeated attempts to isolate the desired dithizone ligands, we concluded that especially the 2-COCH $_3$, NO_2 , OH, and SH derivatives can safely be ruled out as suitable compounds for further investigation.

Most dithizones exhibit two major absorption maxima: the primary band which peaks from 613 and 670 nm, and the secondary band typically from 426 to 492 nm (see Figure 1). When comparing different derivatives, the relative shift of the higher energy absorption band (ca. 450 nm) trails the one at lower energy (>600 nm); i.e., shifts among compounds stay approximately the same for both bands. The colors of all derivatives of dithizone are dark green in solution, except naphthyl dithizone, which is dark blue.

Apart from naphthyl dithizonatophenylmercury, all successfully synthesized mercury dithizonate complexes showed characteristic photochromism, i.e., changing from a shade of orange to blue or blue-purple. This photochromic reaction is best observed in direct African sunlight (at our laboratory), but for the sake of spectroscopy measurements a 400 W mercury "daylight" lamp was used. Figure 2 shows the spectral/color change of the model compound of this investigation, 4-phenoxy dithizonatophenylmercury(II), (4-OPh)DPM, in toluene.

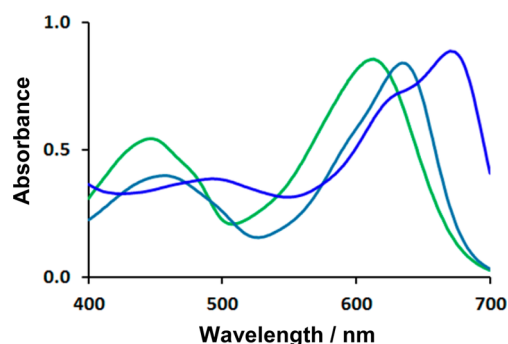


Figure 1. Selected UV-visible spectra of unsubstituted (green), 4-phenoxydithizone (blue-green), and naphthyl dithizone (blue) species in acetone (9×10^{-5} M).

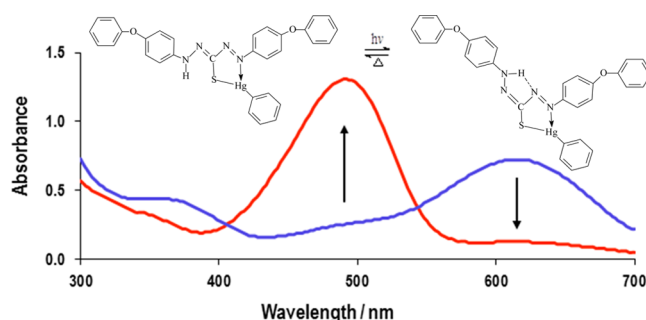


Figure 2. Spontaneous radiationless thermal back-reaction of (4-OPh)DPM in toluene. The blue excited state ($\lambda_{\max} = 615$ nm, $\epsilon = 12\,000$ dm 3 mol $^{-1}$ cm $^{-1}$) reverts back to the orange ground state ($\lambda_{\max} = 490$ nm, $\epsilon = 21\,833$ dm 3 mol $^{-1}$ cm $^{-1}$), with isosbestic points at 406 and 544 nm. The blue spectrum was recorded 5 s after exposure to white light from a 400 W mercury-halide lamp.

Table 2 lists absorbance maxima for all the photochromic complexes of this study. A red-shift of 117 nm is seen during

Table 2. UV-Visible Absorbance Maxima of the Orange Ground States and Blue Photoexcited States of the DPM Series in Acetone

R	λ_{\max} (nm)	
	orange isomer	blue isomer
H	466	583
2-CH $_3$	468	584
4-CH $_3$	478	586
3,4-(CH $_3$) $_2$	480	590
2-OPh	482	606
4-OPh	486	610
naphthyl	489	

the photochromic reaction of the unsubstituted compound, i.e., going from 466 (orange ground/resting state) to 583 nm (blue photoinduced ground state). The corresponding shift is slightly larger for the two phenoxy complexes, namely 124 nm. As for the naphthyl complex, no photochromic behavior could visibly be seen. This, however, does not imply that photoinduced isomerization does not occur; it may simply be too fast to be seen, and in the future this will be established by means of ultrafast laser spectroscopy.

With respect to the unsubstituted complex, absorbance maxima of the phenoxy complexes in acetone are red-shifted by about 20 nm to 486 (orange) and 610 nm (blue). This shift is

slightly less profound when compared to $\Delta\lambda = 43$ nm seen in the previous electronically altered series, where the $-\text{SCH}_3$ substituent caused the largest shift, albeit in dichloromethane.⁷ These figures indicate to what degree of spectral tuning photochromic DPM complexes may be chemically modified, which at this stage is not much. In both studies unsubstituted DPM was observed to absorb at highest energy, i.e., shortest wavelength, with respect to the entire series.

Absorbance maxima of orange (4-OPh)DPM in six solvents—acetone, dichloromethane, tetrahydrofuran, diethyl ether, chloroform, and toluene—using the same concentration (6×10^{-5} M) and temperature (20 °C), are listed in Table 3.

Table 3. UV–Visible Absorbance Maxima of the Orange Ground and Blue Photoinduced States of (4-OPh)DPM in Different Solvents, Arranged in Increasing Order of λ_{max} (Orange)

solvent	λ_{max} (nm)	
	orange isomer	blue isomer
acetone	434	560
DCM	486	604
THF	488	606
diethyl ether	488	608
chloroform	489	602
toluene	490	615

The clear exception in λ_{max} values are those recorded in acetone. In both the orange and blue isomers, relatively large blue-shifts are seen, i.e., from 486 nm in DCM to 434 nm in acetone, with $\Delta\lambda(\text{orange}) = 52$ nm and $\Delta\lambda(\text{blue}) = 44$ nm. All the other solvents gave absorbance maxima narrowly grouped together. Clearly, the polarity of acetone ($\epsilon = 20.7$) may be related to this observation, being more than double that of DCM ($\epsilon = 8.9$); however, in the present series no further relationship is seen between dielectric constants and absorbance maxima in different solvents. Kinetic studies, on the contrary, show a direct relationship between the *rate* of the photochromic return reaction and solvent polarity, as will be seen in the next section.

3.2. Kinetics. To date, no study has been conducted to investigate the effect of steric alterations on the back-reaction of DPM complexes. Apart from the investigation of steric effects, different concentrations, solvents, and temperatures were also involved, and results are reported here.

Care was taken to maintain similar conditions throughout all measurements, since the rate of the back-reaction is sensitive to a number of factors, e.g., similar washing procedures, solvents from similar batches, and use of the same cuvette and instrument.

3.2.1. Substituent. Only six mercury complexes could be employed in this particular investigation, i.e., those which were successfully synthesized and which were visibly photochromic. These included 6×10^{-5} M toluene solutions of sterically altered DPM complexes with dithizonate phenyl ring substituents 4-OC₆H₅-, 2-OC₆H₅-, 3,4-(CH₃)₂-, 4-CH₃-, and 2-CH₃- as well as the unsubstituted complex. Naphthyl-DPM was the only other complex that was successfully synthesized, but for which no visible photochromic reaction was observed.

The rates associated with the plots in Figure 3, as obtained for the spontaneous back-reactions of the above series, are listed in Table 4. The surprising result was that the sterically much larger phenoxy derivatives gave the highest rates. Also,

Table 4. Back-Reaction Rates in Decreasing Order for DPM Complexes under Varying Conditions

	rate, k (s ⁻¹)
Substituent^a	
4-OPh	0.0102
2-OPh	0.0071
H	0.0034
3,4-(CH ₃) ₂	0.0028
4-CH ₃	0.0020
2-CH ₃	0.0004
Concentration (M)^b	
6.0×10^{-5}	0.0065
5.0×10^{-5}	0.0046
4.0×10^{-5}	0.0036
3.0×10^{-5}	0.0027
Solvent^c	
acetone	0.071
tetrahydrofuran	0.046
dichloromethane	0.034
diethyl ether	0.017
chloroform	0.014
toluene	0.009
Temperature (°C)^d	
55	0.0223
45	0.0151
35	0.0110
25	0.0054
15	0.0032
5	0.0019

^a 6.0×10^{-5} M toluene solutions of the substituted series of DPM complexes at 20 °C. ^b(4-OPh)DPM at different concentrations in toluene at 20 °C. ^c 6.0×10^{-5} M (4-OPh)DPM in different solvents at 10 °C. ^d 6.0×10^{-5} M toluene solutions of (4-OPh)DPM at different temperatures.

the rate of the dimethyl complex was seen to be larger than those of the two monomethyl derivatives. The observation that the compounds which were expected to give slower back-reactions due to sterical reasons alone, was initially counter-intuitive. In fact, the phenoxy compound return rates were more than 20 times faster than those of the smaller 2-methyl derivative. Additionally, the latter results are also consistent with rate changes reported in 2013 for studies done in DCM⁷—an agreement between two separate studies which further vindicates the reliability of experimental measurements.

Explanation for this observed trend thus necessarily has to include more aspects than merely steric effects. Electronic effects are not expected to play a significant role, as was recently reported for both UV–visible⁷ and femtosecond laser studies in this field.⁸ Second, based on structural data, H-bonding interactions are also not expected to be of significance here. We thus propose that since the larger molecules have a significantly larger number of vibrational degrees of freedom, the faster reaction rates may largely be attributed to this property. This hypothesis is consistent with the fact that the radiationless back-reaction is essentially thermal by nature, facilitated by intramolecular vibrational modes.

3.2.2. Concentration. Due to the fact that (4-OPh)DPM had not previously been synthesized and thus not kinetically

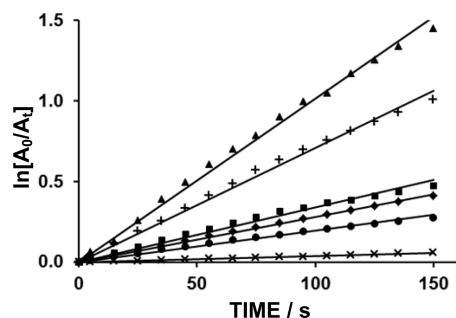


Figure 3. Linear plots of $\ln[A_0/A_t]$ vs time, illustrating first-order kinetics of the spontaneous back-reactions of 6.0×10^{-5} M toluene solutions of the sterically altered DPM series, at 20 °C: 4-OC₆H₅ (▲), 2-OC₆H₅ (+), H (■), 3,4-(CH₃)₂ (◆), 4-CH₃ (●), and 2-CH₃ (×).

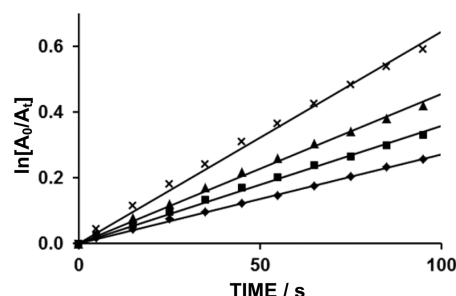


Figure 4. Linear plots of $\ln[A_0/A_t]$ vs time, illustrating first-order kinetics of the spontaneous back-reactions of 6.0×10^{-5} M toluene solutions of (4-Oph)DPM, $T = 20$ °C, at different concentrations: 6×10^{-5} (×), 5×10^{-5} (▲), 4×10^{-5} (■), and 3×10^{-5} M (◆).

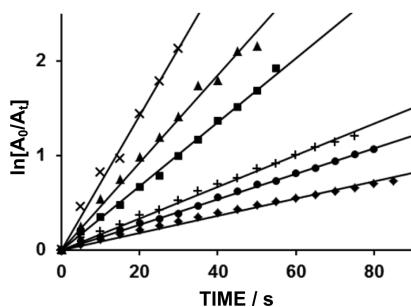


Figure 5. Linear plots of $\ln[A_0/A_t]$ vs time, illustrating first-order kinetics of the spontaneous back-reactions of 6.0×10^{-5} M toluene solutions of (4-Oph)DPM in different solvents at 10 °C, measured at λ_{\max} (blue), for different solvents: acetone (×), THF (▲), DCM (■), diethyl ether (+), chloroform (●), and toluene (◆).

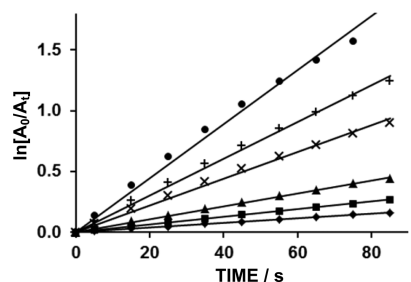


Figure 6. Linear plots of $\ln[A_0/A_t]$ vs time, illustrating first-order kinetics of the spontaneous back-reactions of 6.0×10^{-5} M toluene solutions of (4-Oph)DPM, measured at 615 nm, at different temperatures: 55 (●), 45 (+), 35 (×), 25 (▲), 15 (■), and 5 °C (◆).

investigated, it was selected as model compound in all follow-up investigations. As with the rest, kinetic measurements involving concentration were observed to also follow first-order rates. The linear correlation between absorbance and concentration confirmed adherence to the Beer–Lambert law under all present experimental conditions. Four concentrations were compared, namely 3.0×10^{-5} , 4.0×10^{-5} , 5.0×10^{-5} , and 6.0×10^{-5} M in toluene, while keeping the temperature constant at 20 °C (see Figure 4). The systematic increase in the concentration of (4-Oph)DPM increased the rate of the back-reaction; i.e., doubling the concentration from 3×10^{-5} to 6×10^{-5} M more than doubled the rate, from 0.027 to 0.064 s^{−1}. This is consistent with findings from the earliest kinetic studies done by Meriwether et al. The explanation for this observation is not yet apparent.

3.2.3. Solvent. Solvents are known to have an effect on chemical compound solubility, stability and reaction rates. Correct choice of solvent allows for thermodynamic and kinetic control over chemical reactions. In order to study solvent effect on the lifetime of the photoproduct of (4-Oph)DPM, six solvents were employed—acetone, tetrahydrofuran, dichloromethane, chloroform, diethyl ether and toluene—as representative of a wide range of polarities. This study was done at a lower temperature, namely 10 °C, as the rate of the reaction had to be decreased sufficiently for the faster back-reaction in polar solvents to be observed during the present procedure.

Figure 4 again shows first-order kinetic plots vs time for the photoinduced isomer after exposure to the bright light of a 400 W mercury-halide “daylight” lamp. Corresponding rates are listed in Table 2. Graphical correlations between measured rates and dipole moments, dielectric constants and the molar masses of solvents are shown in Figures 7 and 8. Polar solvents were observed to increase reaction rate, with highest rate in acetone (0.071 s^{−1}, $\epsilon = 20.7$), while the lowest rate was observed in toluene (0.009 s^{−1}, $\epsilon = 2.4$, see Supporting Information for additional data). An almost perfect linear relationship between reaction rate and both dipole moment ($R^2 = 0.93$) and dielectric constant ($R^2 = 0.99$) became apparent, with an 8 times rate increase in acetone over toluene, see Figure 6. THF was excluded as an outlier in the present series, and as such may be ascribed to the coordinating nature of this solvent, or possible H-bonding at the THF oxygen position.

A large increase in solvent polarity for this particular derivative is thus also expected to result in such a high return rate that the photoinduced isomer (blue solution) is no longer visible. This is indeed what was found during ultrafast studies of DPM in polar methanol ($\epsilon = 32.7$), which confirmed the

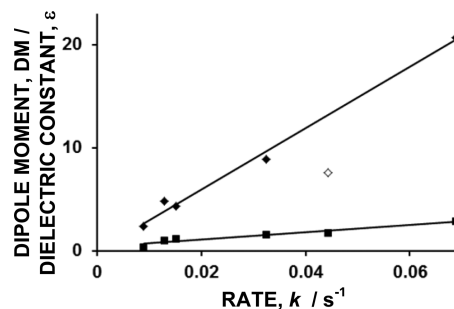


Figure 7. Rate dependence on solvent dielectric constant (◆, $R^2 = 0.99$, excluding THF (◇)) and dipole moment (■, $R^2 = 0.93$) as indicated by the trend lines.

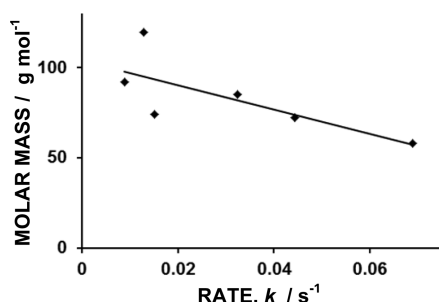


Figure 8. Rate dependence on solvent molar mass as indicated by the trend line.

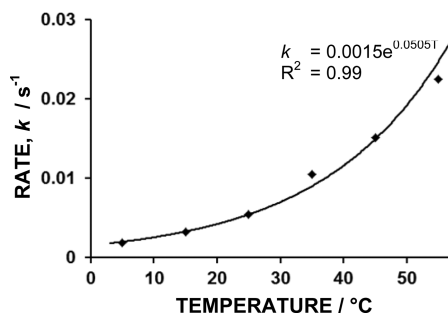


Figure 9. Trend line through the plot of rate constants vs temperature fits an exponential correlation.

photochromic reaction still occurring, but invisible to the naked eye.⁴ The much faster return reaction in polar solvent medium was proposed to proceed via the inversion mechanism, as opposed to the otherwise rotation pathway.⁸

A second factor which intuitively plays a role in the rate of the return reaction in different solvents is the respective molar masses of the different solvents, as also recently reported elsewhere.⁷ Figure 8 illustrates this relationship, which is less precise than when compared to ϵ and DM (Figure 7). Here, with the exception of chloroform and diethyl ether, remaining solvents follow the linear trend closely. The consideration of this correlation to be intuitive is attributed to the higher inertia of heavier surrounding solvent molecules which inhibit vibrational free rotation around the $-C=N-$ bond. In fact, embedding this compound in a clear polymer slows the return reaction to the extent that after illumination the “blue plastic” takes several hours to return to its original orange ground resting state. Thus, a more rigid environment decreases the rate of the back-reaction so that free rotation is significantly inhibited.

3.2.4. Temperature. In order to study the effect temperature has on the return reaction of the photochromic compound, (4-OPh)DPM was dissolved in toluene and rates monitored at six different temperatures—5, 15, 25, 35, 45, and 55 °C—the results of which are shown in Figure 6 and Table 4. Higher temperatures could not be attempted, as the reaction became too fast to accurately measure by means of the present method. On the other hand, temperatures lower than 5 °C resulted in water vapor condensation on the cold cuvette, adversely affecting measurement accuracy.

As the temperature increases from 5 °C ($k = 0.0019 \text{ s}^{-1}$) to 35 °C ($k = 0.0110 \text{ s}^{-1}$), a significant increase in the rate constant is seen, i.e., an almost 6 times increase over a temperature range of 30 °C. Compared to unsubstituted DPM in DCM, which showed a 10 times increase over a temperature

increase of 30 °C,⁷ the (4-OPh)DPM photochromic compound in toluene is thus only about 60% as sensitive to changes in temperature.

Figure 9 shows reaction rate increasing exponentially with temperature, i.e., $k = 0.0015 e^{0.0505T}$. With this expression now established it becomes possible to determine temperatures that are required for specific preset half-lives of the photoinduced blue isomer. For example, at $T = 25 \text{ °C}$ and corresponding $k = 0.0054$ (Table 4), it follows that $t_{1/2} = 128 \text{ s}$ ($t_{1/2} = \ln 2/k$).

In order to slow the reaction down to the point where $t_{1/2} = 1 \text{ day}$, the temperature has to be lowered to -104 °C , as calculated by combining the former equations, i.e.,

$$\ln 2/t_{1/2} = 0.0015e^{0.0505T}$$

Similarly, increasing the temperature to 121 °C will decrease $t_{1/2}$ to 1 s.

The above results reflect findings by Meriwether et al., who observed photochromism in, e.g., lead and cadmium dithizonato complexes only as low as -80 °C and not at room temperature.^{5,6} Also, in the previously reported study involving electronically altered DPM complexes,⁷ related temperatures for unsubstituted DPM were found to be -48 °C ($t_{1/2} = 1 \text{ day}$) and $+91 \text{ °C}$ ($t_{1/2} = 1 \text{ s}$). Comparing these two sets of data, namely the fact that the temperature related to $t_{1/2} = 1 \text{ s}$ is shifted upward by about 30 °C in the 4-OPh complex as compared to DPM, and downward by 56 °C ($t_{1/2} = 1 \text{ day}$), again illustrates the lesser sensitivity of (4-OPh)DPM to changes in temperature.

An increase in temperature ultimately affects the rate at which the product returns to the original ground state. The total bonding energy of the blue isomer ground state is slightly higher than of the orange ground state.⁸ Thermal relaxation to the orange form is inhibited by the large energy barrier in between the two ground states, i.e., at the 90° twist around the $-C=N-$ axis of rotation.⁴ Whereas this barrier is in direction of the forward reaction overcome by vertical excitation onto the S_1 excited-state energy surface, the return path depends on vibrational energy, i.e., heat. From the above kinetic studies it becomes evident to what extent the temperature associated with an increased rate aids the photoinduced ground-state blue molecule to overcome the barrier at the 90° twist angle during back-isomerization.

3.3. X-ray Crystallography. During this investigation attempts were made to grow crystals of all the derivatives of nitroformazan, dithizone and dithizonatophenylmercury, as well as of some of the apparent unsuccessful syntheses products. Although crystalline material was obtained for a number of species, crystal needles of the 2- and 4-phenoxy-nitroformazans (NF) were the only crystals large enough for X-ray data collections. Both crystals were grown from diethyl ether overlaid with hexanes. The structures are shown in Figure 10. See Supporting Information Tables S2–S5 for crystal data, refinement parameters, bond and torsion angles, and bond lengths.

Both compounds yielded monoclinic crystals in the $P2_1/c$ space group ($z = 4$ and 8, respectively). Repeated attempts to grow better crystals of (2-OPh)NF, also by taking crystals directly from the crystallization solvent onto the diffractometer, failed to produce better data for this compound. From the Fourier difference map the (2-OPh)NF phenoxy group was detected as being disordered over two oxygen atoms and was treated as such.

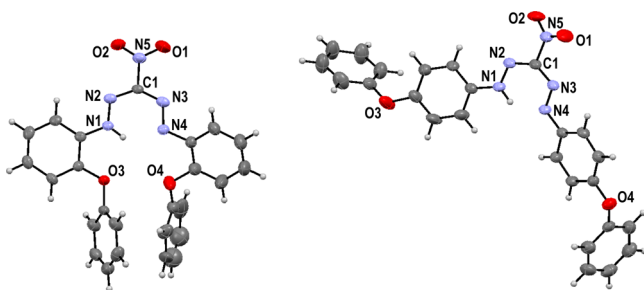


Figure 10. ORTEP views of the X-ray crystal structures of 2-phenoxy-nitroformazan (left) and 4-phenoxy-nitroformazan (right). Thermal ellipsoids are drawn at 50% probability level.

As opposed to the *linear* backbone geometry of dithizone,¹² the nitroformazan precursors adopt a *bent* geometry in the solid state. This bent geometry is held in place by the strong intramolecular hydrogen bond between the (N1)H imine protons and the adjacent N4 atoms in all nitroformazan structures. H-bond distances are in the order of 1.72 Å. Molecular backbones of these molecules are typically flat, except for the phenyl moieties in the substituent, which are twisted out of the plane due to steric obstruction. The nitro-groups at the apex are also slightly twisted with respect to the planar molecular backbone.

As in the case of dithizone, π -electrons along the nitroformazan backbone (N1–N2–C1–N3–N4) are also partially delocalized, with double bonds being longer and single bonds shorter than typically such bonds are otherwise. These properties are in good agreement with published NF structures.^{13–15} Interestingly, the *para*-substituted derivative, (4-OPh)NF, gave similar bond lengths for both the N1–N2 and N3–N4 bonds, which is an indication of the imine proton being shared by atoms N1 and N4. However, the adjacent very slightly shorter C1–N2 bond (1.332 Å), compared to C1–N3 (1.348 Å) shows that this proton may mostly reside on the N1 position. This higher degree of symmetry in (4-OPh)NF, as compared to (2-OPh)NF, is also reflected by its bond angles. The (2-OPh)NF N1–N2–C1 bond angle is almost 4° larger than its N4–N3–C1 angle. This again is ascribed to the imine hydrogen situated on the N1 position. The corresponding angle difference in (4-OPh)NF, where a larger degree of proton sharing between N1 and N4 is deduced, is decreased to just more than 1°.

Interestingly, in both of the *ortho*-substituted compounds, (2-OPh)NF and (2-OMe)NF,¹³ the phenoxy and methoxy substituents on the two phenyl rings are orientated toward each other, with this geometry thus of lower energy than the alternative (when 180° rotated), where the substituents would have been too close to the nitro group oxygens.

See Supporting Information Figures S1 and S2 for projections of molecular packing diagrams.

4. CONCLUSIONS

Limitations during dithizone synthesis are largely ascribed to chemically active substituents which alter the outcome. Substituents on both *ortho*-positions of each dithizone phenyl pose significant steric hindrance during synthesis, while extended aromatic ring systems appear to destabilize the molecule. Single large groups may be utilized, but at the expense of obtaining solid products in some cases. Together with previous studies involving altered electronic substitution

patterns, extended guidelines are now, for the first time, established along which dithizones may in future be synthesized.

Steric effects do not decrease return reaction rates in photochromic mercury complexes—in the traditional sense—but in fact increase the rate due to the increased number of degrees of vibrational freedom in these large molecules, helping overcome the transitional energy barrier. This is consistent with the exponential rate increase with temperature. Linear relationships were found between the rate of the return reaction and solvent properties like dipole moment, dielectric constant, and (roughly) molar mass.

X-ray data of two nitroformazan structures serve as indirect evidence confirming the expected dithizone and mercury complex structures. The mere observation of photochromism in these complexes serves a similar purpose.

■ ASSOCIATED CONTENT

Supporting Information

Table S1, rates of the spontaneous back-reaction of (4-OPh)DPM in various solvents at 10 °C; Table S2, crystal data and refinement parameters of nitroformazan structures; Tables S3–S5, selected bond lengths (Å), bond angles (°), and torsion angles (°); Figures S1 and S2, crystal packing diagrams of 2- and 4-phenoxy-nitroformazan. This material is available free of charge via the Internet at <http://pubs.acs.org>.

■ AUTHOR INFORMATION

Corresponding Author

*Telephone: +27-(0)51-4012923. Fax: +27-(0)51-4446384. E-mail: veschwkg@ufs.ac.za.

Notes

The authors declare no competing financial interest.

■ ACKNOWLEDGMENTS

This work is based upon research supported by the Central Research Fund of the University of the Free State, Bloemfontein, South Africa. LN thanks the South African National Research Foundation (SA-NRF/THRIP), University of the Free State Materials and Nanoscience Research Cluster, SASOL and PETLABS pharmaceuticals for financial support.

■ REFERENCES

- (1) Irving, H.; Andrew, G.; Risdon, E. J. Studies with Dithizone. Part I. The Determination of Traces of Mercury. *J. Chem. Soc.* **1949**, 541–547.
- (2) Webb, J. L. A.; Bhatia, I. S.; Corwin, A. H.; Sharp, A. G. Reactions with Heavy Metals and their Bearing on Poisoning and Antidote Action. *J. Am. Chem. Soc.* **1950**, 72, 91–95.
- (3) Von Eschwege, K. G.; Conradie, J.; Swarts, J. C. A DFT Perspective on the Structures and Electronic Spectra of the Orange and Blue Isomers of Photochromic Dithizonatophenylmercury(II). *J. Phys. Chem. A* **2008**, 112, 2211–2218.
- (4) Schwoerer, H.; Von Eschwege, K. G.; Bosman, G.; Krok, P.; Conradie, J. Ultrafast Photochemistry of Dithizonatophenylmercury(II). *ChemPhysChem* **2011**, 2653–2658.
- (5) Meriwether, L. S.; Breitner, E. C.; Sloan, C. L. Kinetic and Infrared Study of Photochromism of Metal Dithizonates. *J. Am. Chem. Soc.* **1965**, 87, 4441–4448.
- (6) Meriwether, L. S.; Breitner, E. C.; Colthup, N. B. The Photochromism of Metal Dithizonates. *J. Am. Chem. Soc.* **1965**, 87, 4448–4454.

- (7) Von Eschwege, K. G. Synthesis and kinetics of Electronically Altered Photochromic Dithizonatophenylmercury(II) Ccomplexes. *J. Photochem. Photobiol. A: Chem.* **2013**, *252*, 159–166.
- (8) Von Eschwege, K. G.; Bosman, G.; Conradie, J.; Schwoerer, H. Femtosecond Laser Spectroscopy and DFT Studies of Photochromic Dithizonatomercury Complexes. *J. Phys. Chem. A* **2014**, *118*, 844–855.
- (9) Von Eschwege, K. G.; Conradie, J. C.; Kuhn, A. Dithizone and its Oxidation Products—a DFT, Spectroscopic and X-Ray Structural Study. *J. Phys. Chem. A* **2011**, *115*, 14637–14646.
- (10) Von Eschwege, K. G.; Van As, L.; Swarts, J. C. Electrochemistry and spectro-electrochemistry of dithizonatophenylmercury(II). *Electrochim. Acta* **2011**, *56*, 10064–10068.
- (11) Von Eschwege, K. G.; Van As, L.; Joubert, C.; Swarts, J. C.; Aquino, M. A. S.; Cameron, T. S. Intramolecular Interactions in a New *Tris*-Dithizonatocobalt(III) Complex. *Electrochim. Acta* **2013**, *112*, 747–755.
- (12) Laing, M. Dithizone: Redetermination and Refinement of its Crystal Structure. *J. Chem. Soc., Perkin Trans.* **1977**, *2*, 1248–1252.
- (13) Von Eschwege, K. G.; Muller, F.; Hill, T. N. (E)-1-[2-(Methoxyl)phenyl]-2-({(E)-2-[2-(methoxyl)phenyl]hydrazinylidene}-(nitro)methyl)diazene. *Acta Crystallogr.* **2012**, *E68*, o609.
- (14) Von Eschwege, K. G.; Hosten, E. C.; Muller, A. (E)-1-[2-(Methyl)phenyl]-2-({(E)-2-[2-(methyl)phenyl]hydrazinylidene}-(nitro)methyl)diazene. *Acta Crystallogr.* **2012**, *E68*, o425.
- (15) Von Eschwege, K. G.; Muller, F.; Hosten, E. C. (E)-1-[2-(Methylsulfanyl)phenyl]-2-({(E)-2-[2-methylsulfanyl]phenyl]-hydrazinylidene}-(nitro)methyl)diazene. *Acta Crystallogr.* **2012**, *E68*, o199–o200.